Fluorescence Depolarization and Rotational Modes of Tyrosine in Bovine Pancreatic Trypsin Inhibitor†

Andrzej Kasprzak* and Gregorio Weber

ABSTRACT: The fluorescence of bovine pancreatic trypsin inhibitor (BPTI) is due to one or more of its four tyrosine residues. Observations of the stationary polarization of the fluorescence over a large range of temperatures and viscosities permit the demonstration of at least three modes of tyrosine rotation, and perhaps an ultrafast fourth one. The slowest mode is one of motion of the whole molecule; the second, a much faster motion limited to an amplitude of 11°, is not changed by quenching of the fluorescence through addition of citrate and is therefore ascribed to the motion of internal tyrosines of BPTI. The third mode of motion is faster still; it has an amplitude similar to that of the second and, being sensitive to citrate quenching, is attributed to the rotation of the external tyrosine residue. A residual depolarization corresponding to a rotational amplitude of 22° is deduced by comparison of the polarizations of BPTI and tyrosine dissolved in 80% glycerol–water at −40 °C. It is in accord in amplitude with the picosecond tyrosine rotations predicted by Karplus and collaborators from molecular dynamics computer simulations, but it could also originate, in whole or in part, from electronic energy transfer among the tyrosines.

Bovine pancreatic trypsin inhibitor (BPTI)[1] is a compact, disulfide cross-linked peptide chain of small molecular weight containing no tryptophan and four tyrosine residues [for a review, see Laskowski & Sealock (1971)]. Its atomic coordinates have been determined with as good or better precision than those of the other proteins studied by X-ray crystallographic methods (Huber et al., 1974; Deisenhofer & Steigemann, 1975). This circumstance has permitted Karplus and his co-workers application of the methods of molecular dynamics to compute the motions that take place in times on the order of 100 ps (Karplus & McCammon, 1979; Karplus et al., 1980). The rotational motions of the tyrosine residues can be revealed in principle by real-time or stationary-state measurements of fluorescence polarization. The former are particularly difficult because of low quantum yield of the emission (Cowgill, 1967) as well as the short fluorescence lifetimes involved. We have restricted our study to the stationary-state measurements, and as described below, these indicate the existence of a whole spectrum of tyrosine motions.

Materials and Methods

Trypsin inhibitor from bovine pancreas was purchased from Worthington Biochemical Corp. The inhibitor was purified by passage through a G75 Sephadex column (0.9 × 20 cm) equilibrated with 20 mM Bis-Tris buffer, pH 6.5. The fluorescence spectrum of the pure solution could be directly superimposed on the tyrosine fluorescence spectrum, indicating the absence of appreciable tryptophan contamination. Inorganic salts were analytical grade from Baker. Spectrograde glycerol was from Aldrich; L-tyrosine and Bis-Tris were from Sigma. Corrected fluorescence spectra were obtained with a repetitive scanning, photon counting spectrofluorometer (Jameson et al., 1976). Fluorescence titrations were performed with an analogue instrument described by Wehrly et al. (1976). Fluorescence polarization was measured with the photon counting instrument of Jameson et al. (1978). Corrections were introduced for the counts present as solvent background and the difference in optical density of solvent and sample. Each quoted value is an average of at least three independent determinations. Fluorescence lifetimes were obtained by the cross-correlation phase method (Spencer & Weber, 1969) with an SLM 4800 instrument (SLM Instruments Inc., Urbana, IL). Each quoted value of fluorescence lifetime is the average of a set of five to six series of measurements each consisting of 100 samples. The standard deviation for a typical series of measurements was <20 ps. For lifetime and polarization studies, excitation was by 280-nm light isolated by a combination of a monochromator and a Corning 7-54 filter. Baird-Atomic 312-nm interference filters were used to isolate the emission. Because the lifetime of BPTI is below 1 ns, its determination by modulation was not undertaken. BPTI samples in glycerol solutions were made up by adding appropriate aliquots of BPTI in buffer to a preweighed amount of glycerol. Viscosities were obtained from Miner & Dalton (1953).

Results

The fluorescence spectrum of BPTI in pH 6.5 buffer shows a maximum at 305 nm (Figure 1); the fluorescence lifetime is 0.62 ± 0.02 ns. For determination of the contribution of the exposed tyrosine residues to the total emission, quenching studies were carried out. Potassium iodide, sodium acetate, and sodium citrate were found to quench the BPTI fluorescence; potassium chloride has no effect. The most efficient quencher was sodium citrate. The initial portion of the Stern–Volmer plot for citrate quenching has a slope corresponding to an encounter rate greater than 10^{11} M^{-1} s^{-1}. At citrate concentrations greater than 0.05 M, a plateau in the fluorescence efficiency is reached at $F/F(0) = 0.66$ (Figure 2). The fluorescence lifetime at a citrate concentration of 0.12 M is 0.45 ± 0.02 ns. From these figures, it follows that the fluorescence lifetime characteristic of the quenchable residues is 0.99 ns. Glycerol causes an increase in fluorescence yield. In 75% glycerol–pH 6.5 buffer, it is approximately 44%

† From the Department of Biochemistry, Roger Adams Laboratory, School of Chemical Sciences, University of Illinois, Urbana, Illinois 61801. *Received June 10, 1982.* This work was supported by a U.S. Public Health Service grant (GM 11223) to G.W.

* Address correspondence to this author at the Department of Biochemistry and Biophysics, University of California at San Francisco, V.A.M.C., San Francisco, CA 94121.

[1] Abbreviations: BPTI, bovine pancreatic trypsin inhibitor; Bis-Tris, [bis(2-hydroxyethyl)amino]tris(hydroxymethyl)methane.

0006-2960/82/0421-5924$01.25/0

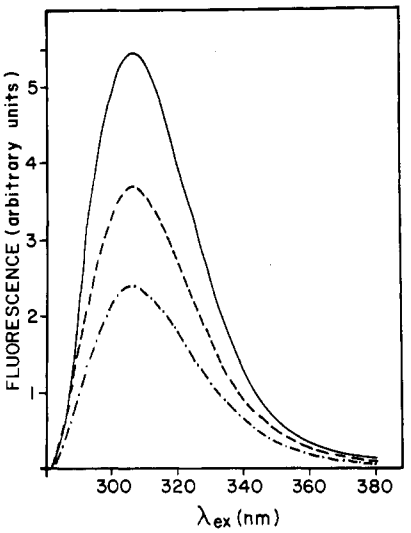

FIGURE 1: Fluorescence spectra of BPTI in Bis-Tris buffer, pH 6.5 (---), in Bis-Tris + 0.12 M citrate (-·-·-), and in 75% glycerol at room temperature (—). The spectra are corrected for grating transmission and detector response. Excitation wavelength, 280 nm.

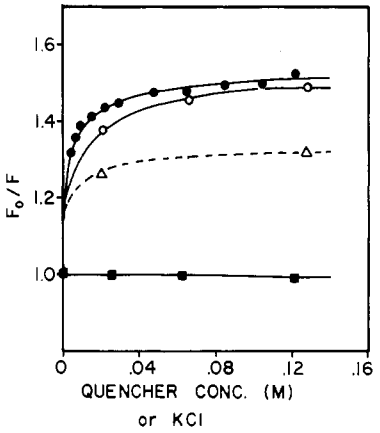

FIGURE 2: Stern–Volmer plots. Effects of citrate and potassium chloride. (●) Citrate in Bis-Tris buffer at 20 °C; (○) citrate in 75% glycerol at 20 °C; (△) citrate in 75% glycerol at −40 °C; (■) KCl in Bis-Tris.

higher than in buffer, and the lifetime is lengthened by 47%. The shape of the fluorescence spectra is identical in both solvents. However, when the glycerol samples are cooled to −40 °C, the fluorescence maximum shifts to 301 nm. Citrate remains an efficient quencher even in glycerol solutions at this temperature (Figure 2). This finding as well as a rate of quenching that is higher than that for diffusion-controlled quenching indicates that the quenching is static, resulting from complex formation between citrate and BPTI tyrosine (Vaughan & Weber, 1970).

Polarization observations were carried out in 75% glycerol–water under the following two conditions: (1) At −40 °C as a function of excitation wavelength, the excitation polarization spectra of citrate-quenched and unquenched samples were identical (Figure 3) with values systematically lower than those of tyrosine in the same solvent. (2) As a function of temperature (Figure 4a), unquenched BPTI yielded a nonlinear Perrin plot; the quenched sample yielded a linear one. Further polarization observations were carried out at 20 °C by varying the glycerol concentration. These yielded a straight line plot (Figure 4b) from which a rotating volume of 5800 mL/mol was derived.

Analysis of Rotational Modes from Perrin Plots. If the values of the anisotropy of emission, A, are plotted against y

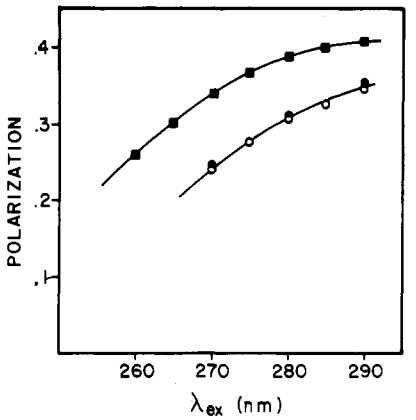

FIGURE 3: Polarization spectrum of l-tyrosine (■) and BPTI (○) and citrate-quenched BPTI (●). All measurements in 75% glycerol at −40 °C.

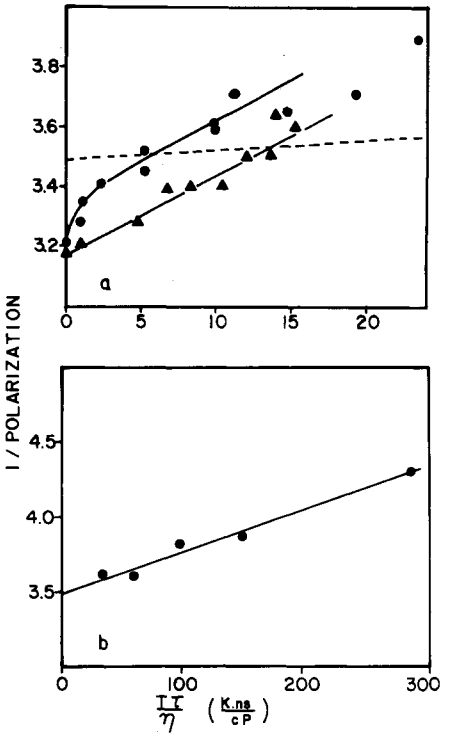

FIGURE 4: Perrin plots for BPTI at high viscosity (a) and low viscosity (b). The solvent in (a) was 75% glycerol and the temperature range was −40 to +55 °C. The solvent in (b) was Bis-Tris buffer with glycerol varied in concentration from 0 to 55%, at 20 °C. The broken line in (a) shows the linear extrapolation of the plot in (b) in the high-viscosity range.

$= RT\tau/\eta$ over an extended range of values of this variable, the graph will be found to consist of segments which can be declared to be, within experimental error, either curved or straight lines. The former usually connect two straight line portions of the plot and do not contain information beyond indicating that two or more modes of rotation are superimposed in their effects. We ignore them in the analysis except when the plot starts at $y = 0$ by such a curved segment. In this case, we use the estimated initial slope as an additional straight line portion of the graph. Each of the straight line regions can be extrapolated back to $y = 0$ to yield an anisotropy which we shall call a "false limiting anisotropy" [FLA(i)]. For that straight line portion of the graph, the Perrin depolarization law takes the form

$$[\mathrm{FLA}(i)/A] - 1 = y/[V(i)] \qquad (1)$$

Table I

extrapolated anisotropy	amplitude (deg)	volume (mL/mol)
$A(0) = 0.2971$	22	
$FLA(1) = 0.2346$	11	900
$FLA(2) = 0.2214$	10	19
$FLA(3) = 0.2108$	unlimited	5900

$V(i)$ is the apparent volume to be assigned to the rotating unit carrying the fluorophore. From this value of $V(i)$, a rotational rate or rotational relaxation time can be calculated for a fixed value of temperature/viscosity. If the slope of the slowest mode of rotation (highest values of y) is appreciable, this mode may be taken as one of unlimited amplitude of rotation. The faster modes represented by other straight segments of the graph are modes of limited rotational amplitude, AMP(i), which is estimated by means of the relation

$$\mathrm{FLA}(i)/[\mathrm{FLA}(i+1)] = 2/\{3\cos[\mathrm{AMP}(i)]^2 - 1\} \quad (2)$$

where FLA(i) is the false limiting anisotropy for the mode concerned and FLA($i + 1$) the one corresponding to the next slower mode. Equation 2, according to Soleillet (1929), assumes spherically symmetric free rotations, a case evidently different from that of the rotations of tyrosine limited by the interactions with the surroundings. In this latter case, we expect the rotations to be both anisotropic and inhomogeneous, but eq 2 seems to us an adequate approximation for obtaining an estimate of the mean amplitude of rotation and for comparative purposes. When the experimental data for BPTI are subjected to this analysis, one can distinguish three different rotational modes, as depicted in Figure 4 and Table I. $A(0)$ is the anisotropy of the emission from tyrosine in the same solvent at −40 °C, which we take to be the true limiting anisotropy. Comparison of the largest extrapolated anisotropy of BPTI, quenched or unquenched [FLA(1) in Table I], with that of tyrosine, at −40 °C in 75% glycerol–water, indicates in the former a residual depolarization corresponding to an angle of 22° between the oscillators of absorption and emission. This may be interpreted as arising from local rotations of the tyrosine residues or from transfer of the excitation among the four tyrosines in BPTI. In this latter case, a fraction of the excitations would be followed by emission from a differently oriented residue. Let f(ee) and f(ie) be the fractions of the total emission due to the external (quenchable) residues following the excitation of external and internal residues, respectively, while f(ei) and f(ii) are the corresponding quantities for the internal (unquenchable) residues. Let A_{int} stand for the anisotropy of the emission by the internal tyrosines when unconnected to the external ones, and A_{ext} is the corresponding quantity for these latter residues. Let A'_{int} be the anisotropy emitted by the internal residues after excitation of the external ones and A'_{ext} the anisotropy corresponding to the converse process. Then, the anisotropy before quenching is

$$A = \{Q_{ext}[A_{ext}f(\mathrm{ee}) + A'_{ext}f(\mathrm{ie})] + Q_{int}[A_{int}f(\mathrm{ii}) + A'_{int}f(\mathrm{ei})]\}/\{Q_{ext}[f(\mathrm{ee}) + f(\mathrm{ie})] + Q_{int}[f(\mathrm{ei}) + f(\mathrm{ii})]\} \quad (3)$$

where Q_{ext} and Q_{int} are fluorescence efficiencies. When the fluorescence from external residues is quenched

$$Q_{ext} = 0 \qquad f(\mathrm{ei}) = 0 \quad (4)$$

the anistropy becomes

$$A = A_{int}$$

and

$$Q_{ex}f(\mathrm{ee})(A_{int} - A_{ext}) + Q_{in}f(\mathrm{ei})(A_{int} - A'_{int}) + Q_{ex}f(\mathrm{ie})(A_{int} - A'_{ext}) = 0 \quad (5)$$

The middle term in eq 5 is necessarily positive since we assume that energy transfer is the cause of the depolarization. If there is a single quenched external residue as is the case in BPTI, the first term in eq 5 is negative, and the third may be positive or negative. In qualitative fashion, if the anisotropy of the external residues is higher than that of the internal ones, when the former is quenched the anisotropy ought to fall, but this fall may be compensated by the decrease in the indirect excitation of the internal residues. If there is exact compensation, the anisotropy observed at −40 °C remains unchanged after the external residues are quenched. On the other hand, if external and internal residues have similar freedom of local rotation, quenching would leave the anisotropy also unchanged.

When the temperature is raised from −40 °C, quenched and unquenched solutions show different anisotropies (Figure 4a). The Perrin plot of the unquenched solution is curved toward the abscissa, indicating the existence of two comparable relaxation times, of which the slowest is the only one discernible in the quenched solution. The conclusion must be that the external tyrosine has an additional mode of temperature- (and viscosity?) dependent rotation. From the extrapolation of the linear portion of the plot of the unquenched solution to infinite viscosity, one can estimate that this additional angular amplitude of motion of the external tyrosine is ca. 10° and corresponds to a volume of about 19 mL. The Perrin plot for solutions of BPTI at 20 °C and higher temperatures (Figure 4b) shows, on the other hand, the expected behavior for a compact molecule of volume ca. 6000 mL/mol. Thus, from the observations at the various temperatures, at least three modes of rotation are seen: a slow one corresponding quite well to the molecule as a whole, a much faster mode limited to an amplitude of some 11° which is attributed to the internal tyrosines and which may be temperature and viscosity dependent, or only temperature dependent, and an even faster, restricted motion of about 10° of the external tyrosine alone. The difference in polarization between tyrosine and BPTI in the vitrified solvent (glycerol–water at −40 °C) may arise from a fourth ultrafast mode of tyrosine rotation in BPTI that precedes these three, but with the present evidence, we cannot exclude that the depolarization from which we deduce it results from electronic energy transfer among the four tyrosines.

In conclusion, an examination of the dependence of the anisotropy upon the temperature discloses the presence of several modes of partial rotation. If a shorter range of values of temperature and/or visocity is employed, one can easily miss the presence of one or another of them. The observations show that the depolarization of the fluorescence emitted by the tyrosines is determined in a complex fashion by the various rotational modes of the molecule and that additionally the distinction between depolarization by rotation and by electronic energy transfer among similar residues is not always an easy one to make. In principle, it should be possible to distinguish between the two by excitation at the red edge of the absorption spectrum of the fluorophore as it is known that energy transfer among like residues does not take place under these circumstances (Weber & Shinitzky, 1970). We did not find it possible to apply this test practically to BPTI on account of the very low quantum yield. The signal to noise ratio on red-edge excitation was too small to permit a reliable analysis of the polarization values.

If the initial depolarization of 22° is due to a rotational motion of the tyrosines, it must be accomplished in a small

fraction of the lifetime. Original computations of McCamon and Karplus employing the methods of molecular dynamics predict restricted tyrosine motions of this amplitude with a quasi-harmonic character completed in picosecond times. A more detailed explicit analysis of the resulting depolarization of the fluorescence has been carried out by Levy & Szabo (1982), who show that stable depolarization values would be reached in about 2 ps. The present observations register the expected short-time depolarization but cannot unequivocally exclude energy transfer among the tyrosines as a partial or unique contribution to this effect. It is of interest to note that if the fast depolarization is assumed to be wholly due to the rotations of the tyrosines, the ratio $FLA(1)/A(0)$ observed, 0.78, virtually coincides with the average value resulting from the ultrafast motion of the four tyrosines calculated by Levi & Szabo (1982) for one of their models [see second column of Table I of Levi & Szabo (1982)]. A compact protein molecule with a single tyrosine will be required to test the predictions of molecular dynamics. This appears as a worthwhile undertaking because the analysis of the fast motions of proteins by this method offers considerable promise, and an experimental verification of some of its basic predictions would enlarge its scope and increase confidence in its application.

References

Cowgill, R. W. (1967) *Biochim. Biophys. Acta 140*, 552–554.

Deisenhofer, J., & Steigemann, W. (1975) *Acta Crystallogr., Sect. B B31*, 238–250.

Huber, R., Kikla, D., Bode, W., Schwager, P., Bartels, K., Deisenhofer, W., & Steigemann, W. (1974) *J. Mol. Biol. 89*, 73–101.

Jameson, D. M., Spencer, R. D., & Weber, G. (1976) *Rev. Sci. Instrum. 47*, 1034–1038.

Jameson, D. M., Weber, G., Spencer, R. D., & Mitchell, G. W. (1978) *Rev. Sci. Instrum. 49*, 510–514.

Karplus, M., & McCammon, J. A. (1979) *Nature (London) 277*, 578–579.

Karplus, M., Gelin, B. R., & McCammon, J. A. (1980) *Biophys. J. 32*, 603–618.

Laskowski, M., Jr., & Sealock, R. (1971) *Enzymes, 3rd Ed. 3*, 375–473.

Levy, R. M., & Szabo, A. (1982) *J. Am. Chem. Soc. 104*, 2073–2075.

Miner, M., & Dalton, N. N. (1953) *Glycerol*, pp 246–286, Reinhold, New York.

Soleillet, P. (1929) *Ann. Phys. (Paris) 12*, 23–79.

Spencer, R. D., & Weber, G. (1969) *Ann. N.Y. Acad. Sci. 158*, 361–367.

Vaughan, W. M., & Weber, G. (1970) *Biochemistry 9*, 464–473.

Weber, G., & Shinitzky, M. (1970) *Proc. Natl. Acad. Sci. U.S.A. 65*, 823–830.

Wehrly, J. A., Williams, J. F., Jameson, D. M., & Kolb, D. A. (1976) *Anal. Chem. 48*, 1424–1426.

A New Method To Characterize the Translation Initiation Sites of Messenger Ribonucleic Acids†

James R. Pease,‡ David W. Leung,§ and John M. Clark, Jr.*

ABSTRACT: RNA can be radiolabeled in vitro with ^{125}I in uridine and cytidine residues by initial mercuration of these pyrimidine residues by the method of Dale et al. [Dale, R. M. K., Martin, E., Livingston, D. C., & Ward, D. C. (1975) *Biochemistry 14*, 2447–2457] and subsequent electrophilic displacement of the mercury with $^{125}I^+$ generated by the method of Commerford [Commerford, S. L. (1971) *Biochemistry 10*, 1993–2000]. These two reactions can be manipulated to produce intact high specific activity ^{125}I-labeled mRNA containing approximately equal specific activity in their 5-[^{125}I]iodouridine and 5-[^{125}I]iodocytidine residues. In vitro radiolabeling of satellite tobacco necrosis virus RNA (STNV RNA) by this procedure yields a ^{125}I-labeled mRNA that is biologically active in ribosome protection analyses in that one obtains the correct translation initiation fragments of the mRNA. Exhaustive digestion of a specific ^{125}I-labeled 32 nucleotide long initiation fragment of STNV RNA using four separate nucleotide-specific digestion (hydrolysis) reactions yields four different populations of ^{125}I-labeled digestion products that can be resolved by two-dimenstional fingerprint procedures. Characterization of all these ^{125}I-labeled digestion products followed by overlap nucleotide sequence comparisons of these specific digestion products allows a nucleotide sequence determination of the original 32 nucleotide long translation initiation fragment of this mRNA. This suggests that this overall in vitro procedure can be used to determine the nucleotide sequence of the translation initiation site(s) of any mRNA.

Ribosome protection analyses of the nucleotide sequence of the translation initiation site(s) of mRNAs (Steitz, 1969) require high specific activity mRNAs with uniformly distributed radiolabel(s). Messenger RNAs derived from single cell or tissue culture systems are ideally suited for such analyses for one can usually prepare high specific activity uniformly radiolabeled mRNAs from such systems by in vivo labeling with $^{32}P_i$ or combinations of other nucleic acid precursors. In contrast, many multicelled or whole organism systems have slow growth rates or endogenous pools of nucleic acid precursors that restrict in vivo radiolabeling procedures. The resultant lack of uniformly radiolabeled, high specific activity

† From the Biochemistry Department, University of Illinois, Roger Adams Lab, 1209 W. California St., Urbana, Illinois 61801. *Received May 24, 1982.* This work was supported by U.S. Public Health Service Grant GM-08647.

‡ Present address: P-L Biochemicals, Milwaukee, WI 53207.

§ Present address: Genentech Co., South San Francisco, CA 94080.

0006-2960/82/0421-5927$01.25/0